J Neurosurg 93:658–666, 2000

Products of hemolysis in the subarachnoid space inducing spreading ischemia in the cortex and focal necrosis in rats: a model for delayed ischemic neurological deficits after subarachnoid hemorrhage?

JENS P. DREIER, M.D., NATALIE EBERT, JOSEF PRILLER, M.D., DIRK MEGOW, PH.D., UTE LINDAUER, D.V.M., ROLF KLEE, M.D., UWE REUTER, M.D., YOSHINORI IMAI, M.D., KARL M. EINHÄUPL, M.D., ILYA VICTOROV, M.D., AND ULRICH DIRNAGL, M.D.

Department of Neurology and Physiology, Charité, Humboldt-University, Berlin, Germany; Laboratory of Experimental Neurocytology, Brain Research Institute, Moscow, Russia; and Department of Neurochemistry, National Institute of Neuroscience, Tokyo, Japan

Object. The pathogenesis of delayed ischemic neurological deficits after subarachnoid hemorrhage has been related to products of hemolysis. Topical brain superfusion of artificial cerebrospinal fluid (ACSF) containing the hemolysis products K^+ and hemoglobin (Hb) was previously shown to induce ischemia in rats. Superimposed on a slow vasospastic reaction, the ischemic events represent spreading depolarizations of the neuronal–glial network that trigger acute vasoconstriction. The purpose of the present study was to investigate whether such spreading ischemias in the cortex lead to brain damage.

Methods. A cranial window was implanted in 31 rats. Cerebral blood flow (CBF) was measured using laser Doppler flowmetry, and direct current (DC) potentials were recorded. The ACSF was superfused topically over the brain. Rats were assigned to five groups representing different ACSF compositions. Analyses included classic histochemical and immunohistochemical studies (glial fibrillary acidic protein and ionized calcium binding adaptor molecule) as well as a terminal deoxynucleotidyl transferase–mediated deoxyuridine triphosphate nick-end labeling assay.

Superfusion of ACSF containing Hb combined with either a high concentration of K^+ (35 mmol/L, 16 animals) or a low concentration of glucose (0.8 mmol/L, four animals) reduced CBF gradually. Spreading ischemia in the cortex appeared when CBF reached 40 to 70% compared with baseline (which was deemed 100%). This spreading ischemia was characterized by a sharp negative shift in DC, which preceded a steep CBF decrease that was followed by a slow recovery (average duration 60 minutes). In 12 of the surviving 14 animals widespread cortical infarction was observed at the site of the cranial window and neighboring areas in contrast to findings in the three control groups (11 animals).

Conclusions. The authors conclude that subarachnoid Hb combined with either a high K^+ or a low glucose concentration leads to widespread necrosis of the cortex.

KEY WORDS • ischemia • vasospasm • migraine • hemoglobin • rat

INDUCTION of focal cerebral ischemia by hemolysis products in the subarachnoid space has been hypothesized to explain the pathogenesis of DINDs after SAH.[26,49] During the course of hemolysis, important extracellular changes include release of Hb and K^+.[36,37,40] Neither of these factors alone generates ischemia.[48] However, topical brain superfusion of ACSF containing Hb combined with a high concentration of K^+ (35 mmol/L) led to a low flow state superimposed with acute, spreading decreases in CBF in rats in which a cranial window had been made.[9] The spread of decreases in CBF provided an argument that the decreases were the result of a disturbed CBF response to CSD. Another argument was that CSD is known to be induced by both high concentrations of extracellular K^+ and low flow states.[4,20,32] In additional experiments, distantly elicited CSDs moved to the site of the cranial window, where they induced a normal spreading hyperemia in the presence of normal ACSF. In contrast, CSDs induced spreading decreases in CBF when ACSF containing K^+ at a concentration of 20 mmol/L was superfused combined with either the NO scavenger Hb or the NOS inhibitor L-NNA.[9] Intravenous infusion of the vasodilator nimodipine (2 μg/kg/min) retransformed the spreading decreases in CBF into normal cortical spreading hyperemias.[9] The decreases in CBF seemed to be associated with energy deficiency because: 1) CBF dropped below the ischemic threshold; 2) the negative DC shift was prolonged in comparison with a normal CSD; and 3) a pat-

Abbreviations used in this paper: ACSF = artificial cerebrospinal fluid; CBF = cerebral blood flow; CSD = cortical spreading depression; CSF = cerebrospinal fluid; CSI = cortical spreading ischemia; DC = direct current; DIND = delayed ischemic neurological deficit; GFAP = glial fibrillary acidic protein; Hb = hemoglobin; Iba1 = ionized calcium binding adaptor molecule; LD = laser Doppler; L-NNA = *N*-nitro-L-arginine; NMDA = *N*-methyl-D-aspartate; NO = nitric oxide; NOS = NO synthase; SAH = subarachnoid hemorrhage; TUNEL = terminal deoxynucleotidyl transferase–mediated deoxyuridine triphosphate nick-end labeling.

tern of O_2 free radical production characteristic of transient ischemia was seen.[9] Therefore, the histopathological outcome after spreading ischemia was analyzed in the present study. We also tested whether spreading ischemia is produced by ACSF containing Hb and a low concentration of glucose because a low concentration of glucose is also known to induce CSD[1,50] and was found to decrease in the brain cortex before DINDs after SAH in humans.[34,42]

Materials and Methods

Animal Preparation

All animal experiments were approved by the Landesamt für Arbeitsschutz, Gesundheitsschutz und technische Sicherheit Berlin (G 0346/98). Thirty-one male Wistar rats, weighing 250 to 300 g each, were anesthetized with 1.5% halothane in a mixture of 30% O_2/70% N_2O. The tail artery was cannulated and a continuous intravenous infusion of saline solution (1 ml/hour) was administered. Body temperature was maintained at 38 ± 0.5°C by using a heating pad. Systemic arterial pressure was monitored and the rats' PaO_2, $PaCO_2$, and pH were measured serially by using a blood gas analyzer. The depth of anesthesia was monitored by blood pressure control and response to tail pinching.

A craniotomy measuring 2 × 3 mm was performed at the frontal suture by using a saline-cooled drill. The dura mater was removed and a closed cranial window was implanted. The cortical surface under the window was superfused continuously with ACSF. The composition of the ACSF in millimoles per liter was: Na^+ 152, K^+ 3, Ca^{++} 1.5, Mg^{++} 1.2, HCO_3^- 24.5, Cl^- 135, glucose 3.7, and urea 6.7. The ACSF was equilibrated with a gas mixture containing 6.6% O_2, 5.9% CO_2, and 87.5% N_2, leading to a PO_2 of 118.3 ± 14.2 mm Hg, a PCO_2 of 34.5 ± 3.9 mm Hg, and a pH of 7.37 ± 0.09. After implantation of the cranial window, the animals' wounds were treated with lidocaine HCl gel (2%) and sutured. The rats were allowed to awaken after disconnection of the cranial window from the syringe pump. The opioid agent, buprenorphine (0.5 mg/kg body weight), was administered subcutaneously as a postoperative analgesic agent. The animals recovered quickly. They drank and groomed on the 1st postoperative day.

Experiments were performed on the 2nd postoperative day after anesthesia had been induced by an intraperitoneal injection of thiopental sodium (Trapanal, 90 mg/kg body weight). Usually, one injection of thiopental sodium was sufficient for the entire experiment. The animals continued to be sedated for several hours after the experiment. They drank and groomed on the 1st postexperimental day, at which time they were examined neurologically and graded according to the scale of Menzies, et al.[29] The rat brains were fixed by transcardial perfusion 24 (three animals) or 48 hours (22 animals) after the experiment.

Experimental Paradigm

To induce CSI, topical brain superfusion was performed using ACSF containing Hb (2 mmol/L) combined with K^+ (35 mmol/L) in 16 animals. In another four animals, ACSF containing Hb (2 mmol/L) and glucose (0.8 mmol/L) was superfused to induce CSI.

The control animals received ACSF containing Hb (2 mmol/L) combined with normal levels of K^+ and glucose (three animals); no Hb but increasing concentrations of K^+ (35, 50, and 80 mmol/L) and normal levels of glucose (five animals); and no Hb but normal levels of K^+ and glucose at a concentration of 0.8 mmol/L (three animals). Washout with physiological ACSF was initiated after 3 hours in all experiments.

The experimental K^+ concentrations (3, 35, 50, and 80 mmol/L) determined the Na^+ concentrations (152, 120, 105, and 75 mmol/L, respectively) in the ACSF. Hemoglobin was freshly prepared from heparinized arterial blood of Wistar rats. The blood was centrifuged (2500 G, 5 minutes, 4°C) and the plasma was discarded. The cells were washed five times with three to four volumes of cold 0.9% NaCl, and the buffy coat was removed. The cells were lysed by sonication. The suspension of lysed cells was subjected to centrifugation (15,000 G, 10 minutes, 4°C) and the pellet was removed. The Hb-containing supernatant was transferred by gel chromatography to the ACSF. Both the concentration and composition of the Hb were measured using a radiometer (total Hb 2 ± 0.3 mmol/L; oxyHb 95.4 ± 2%; COHb 2.2 ± 1.2%; metHb 2.4 ± 1.9%; deoxyHb 0 ± 0%; O_2 saturation 100%).

Data Collection and Statistical Analysis

Cerebral blood flow was monitored continuously by using two LD flow probes. One LD probe was positioned in the caudal and the other in the rostral third of the cranial window. The spatial resolution of the LD probes is approximately 1 mm^3.[8] The DC potential was recorded at the cranial window by implementing a silver–silver chloride wire with an agar bridge inserted into the space between the cortex and the coverslip. The electrode was right next to the caudal LD probe; the wire was connected to an amplifier. The rats' body temperature, CBF, and DC potential were recorded continuously by using a personal computer and a chart recorder.

Changes in CBF were calculated in relation to baseline at the onset of the experiment (baseline = 100%). All data presented in text, tables, and figures are expressed as the mean values ± standard deviation.

Histological Study

The rat brains were fixed by transcardial perfusion with modified Lillie fixative[24] (absolute alcohol [70%], 37% formalin [20%], glacial acetic acid [10%]). After perfusion each brain was refrigerated in situ overnight in the same fixative. Thereafter, the brain was removed from the skull. Dissected brains were treated with 96% alcohol overnight before being paraffin embedded according to a routine procedure. Eight- to 10-micrometer coronal or sagittal sections were mounted on slides treated with albumin and stained using cresyl violet, hematoxylin and eosin, and vanadium acid fuchsin–toluidine blue methods.[47] Coronal sectioning was begun 2 mm from the herniated window area. Sagittal sections were cut from complete hemispheres. Several sections were obtained every 200 μm. Immediately neighboring sections were stained using the various histochemical and immunohistochemical methods so that direct comparisons were possible. All cerebral structures in the sections were carefully evaluated by a neuropathologist.

Immunohistochemical Analysis and TUNEL Assay

Immunohistochemical analysis was performed in the manner described by Priller, et al.[41] Briefly, after deparaffinization of the tissue, primary antibodies (anti-GFAP and anti-Iba1[18]) were added overnight. A secondary biotinylated goat/anti–rabbit antibody was applied for 1 hour at room temperature, and visualization was achieved using the avidin–biotin complex method. Anti-Iba1 antibody specifically recognizes microglia and cells of monocytic lineage.[18] The TUNEL assay was performed using a commercially available kit with only a slight modification made to the manufacturer's protocol.

Sources of Supplies and Equipment

Systemic arterial pressure was monitored using an RFT Biomonitor, obtained from VEB Messgeraetewerk (Zwoenitz, Germany). The Compact 1 blood gas analyzer was purchased from AVL Medizintechnik GmbH (Bad Homburg, Germany). Lidocaine HCl was acquired from Astra GmbH (Wedel, Germany), buprenorphine from Boehringer-Mannheim (Mannheim, Germany), and thiopental Na (Trapanal) from BYK Pharmaceuticals (Konstanz, Germany). Gel chromatography was performed using Bio-Gel P-6, manufactured by BioRad (Hercules, CA). The LD probes were obtained from Perimed AB (Järfälla, Sweden) and the amplifier from Jens Meyer (Munich, Germany). The DASH IV chart recorder was purchased from Astro-Med, Inc. (West Warwick, RI). The anti-GFAP was obtained from Dako Corp. (Carpinteria, CA). The avidin–biotin complex method was performed using the Vectorstain ABC kit manufactured by Vector Laboratories (Burlingame, CA), and the complex reacted with 3,3′diaminobenzidine/H_2O_2 purchased from

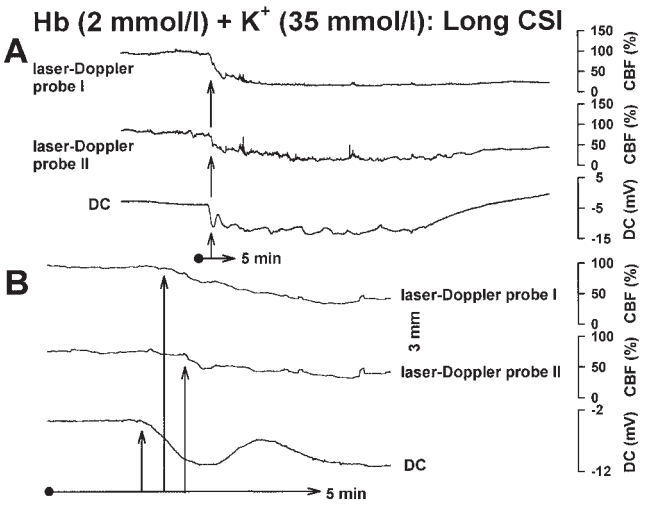

FIG. 1. A: Traces showing that CSI originates in the cerebral cortex during superfusion of ACSF containing Hb (2 mmol/L) and K^+ (35 mmol/L). The onset of CSI is indicated by the *arrows*. The CSI event is characterized by a sharp negative shift in DC and a steep decrease in CBF. In this case, the negative shift in the DC and the decrease in CBF lasted for more than 30 minutes. Note the waveform of DC negativity, which represents multiple CSD cycles. B: Traces showing a higher temporal resolution of the onset of CSI. Note that the negative shift in DC precedes the decrease in CBF measured by LD Probes I and II. (The DC electrode was positioned close to Probe I.) Compare also the similarity between the initial segment of the negative DC shift with that of a CSD during superfusion of ACSF with K^+ (80 mmol/L) and without Hb (Fig. 8B).

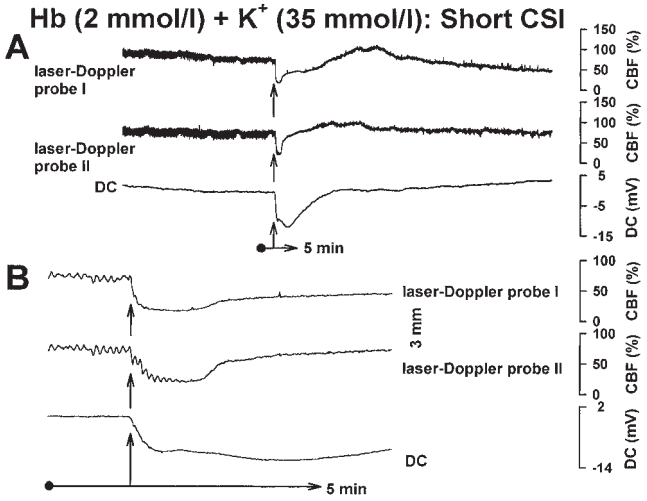

FIG. 2. A: Traces obtained in another animal demonstrating a shorter episode of CSI under the same conditions as those described in Fig. 1. The shorter duration is likely responsible for the lack of tissue damage in this animal. The duration of CSI was heterogeneous interindividually (compare Figs. 1 and 2) and intraindividually (compare with Fig. 6). B: Traces showing a higher temporal resolution of the onset of CSI, revealing that DC negativity and CBF decreases began almost simultaneously in this animal. The fluctuations before the CSI event represent vasomotion, which is blocked afterward.

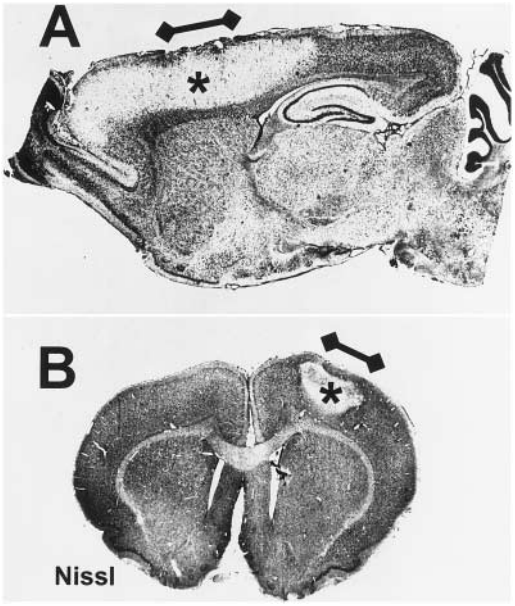

FIG. 3. Panoramic views of sections through complete rat brain demonstrating CSI after superfusion of the brain with ACSF containing Hb (2 mmol/L) and K^+ (35 mmol/L) induced cortical infarction. The two panoramic photographs were obtained in two different animals, and each shows a cortical area neighboring the cranial window 48 hours after CSI was initiated. *Bars* indicate positions of cranial windows and *asterisks* focal areas of cortical necrosis. A: Sagittal section. Note that the necrosis is larger than the window. Original size of section is 1.5 cm from frontal tip of cerebrum to occipital tip of cerebrum. B: Coronal section. Cresyl violet (Nissl) staining. Original size of section is 1.4 cm from left to right.

Sigma Chemicals (Deisenhofen, Germany). The TUNEL assay was performed using the Apoptag kit manufactured by Intergen (Oxford, UK).

Results

Physiological parameters were within normal limits during preparation of the cranial window. Brain herniation into the window area and meningeal reactions were observed in all animals histologically. The meningeal changes consisted of invasion of neutrophils without parenchymal damage. The meningeal reaction was found in both hemispheres but was more pronounced on the side ipsilateral to the injury.

Experimental Animals

Superfusion of ACSF containing Hb (2 mmol/L) and K^+ (35 mmol/L) reduced CBF to a level of 65 ± 25% compared with baseline (baseline = 100%). An episode of CSI appeared 49 ± 23 minutes after onset of superfusion (Fig. 1). They were characterized by a negative shift in DC and a steep decrease in CBF. The DC negativity either preceded the CBF decrease (Fig. 1B) or both started almost simultaneously (Fig. 2B). The CBF decrease never preceded the DC shift. The amplitude of the DC shift was −10.9 ± 3.5 mV. The DC shift lasted for 23 ± 12 minutes. Cerebral blood flow decreased to 22 ± 9%. Recovery of CBF occurred gradually. The CBF level before

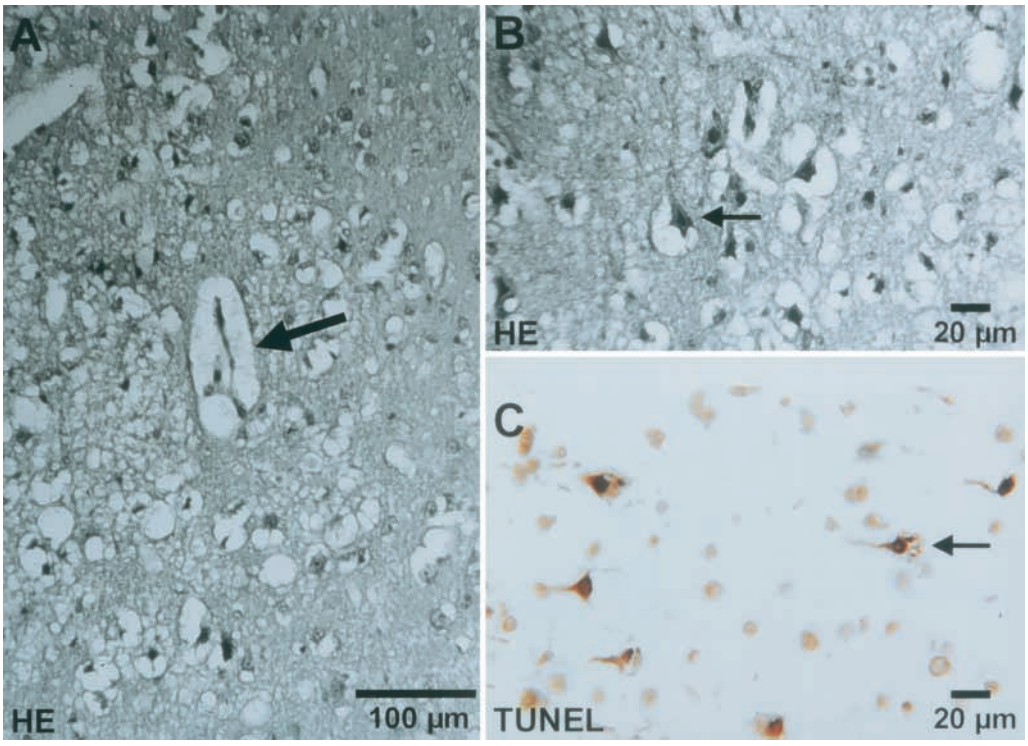

FIG. 4. Photomicrographs. A: Focal cortical necrosis 24 hours after CSI was induced by ACSF containing Hb and K^+ (35 mmol/L). Note the perivascular spongiform changes and necrotic neurons with perineuronal halos. H & E. (An almost identical figure was presented in Fig. 2 of the article by Neil-Dwyer, et al., to illustrate changes after DINDs following SAH in humans.) B: Higher magnification of the tissue sample shown in A reveals shrunken, hyperchromatic, acidophilic, necrotic neurons with perineuronal halos *(arrow)*. H & E. C: Results of staining of cells in the cortex 48 hours after CSI was induced. Positively staining neurons can represent either necrosis or apoptosis. TUNEL staining.

onset of the CSI event was reached after 63 ± 42 minutes. One to four episodes of CSI occurred during an observation period of 3 hours.

Five animals died within hours after the experiment; 11 animals survived. Hemiparesis was observed in nine of these 11 animals 24 hours after the experiment (average grade 2.4 ±1.6 on a scale ranging from 0 [no deficit] to 4 [severe paresis]). Histological analysis revealed cortical brain infarction in nine of the 11 animals. The localization and extent of the infarct is illustrated in Fig. 3. The infarcted area was larger than the area of the cranial window (Fig. 3A) in the majority of animals. Necrosis was present in all cortical layers. White matter adjacent to the cortex was occasionally involved (data not shown). Larger magnification of tissue samples revealed perivascular spongiform changes (Fig. 4A) and shrunken, hyperchromatic, acidophilic neurons with perineuronal halos (Fig. 4B). Cells that were TUNEL positive and ball-shaped cellular fragments were also found after CSI was induced (four animals). Most of them were observed in the outer zone of the infarcted area and its surroundings. The main fraction of TUNEL-positive cells represented damaged neurons, as shown in Fig. 4C. Staining with GFAP revealed loss of astrocytes that was confined to the infarcted area (four animals; Fig. 5Aa). Astrocytes were activated all over the remaining brain, including the contralateral hemisphere. Staining with Iba1 revealed activated microglial cells in both hemispheres (four animals). Large numbers of phagocytic microglia and other macrophages were observed in the infarcted zone (Fig. 5Ba). In two animals, no necrosis developed. The time between CBF decrease and complete recovery ranged between 2 minutes and 13 minutes in these animals (Fig. 2A), which was significantly shorter than the time that elapsed in the other nine animals (Fig. 1A).

Artificial CSF containing Hb (2 mmol/L) combined with K^+ (physiological level) and glucose (0.8 mmol/L) also induced CSI (four animals). Data from a complete experiment are shown in Fig. 6. As was the case with the combination of Hb and a high concentration of K^+ in ACSF, the combination of Hb and a low concentration of glucose in ACSF reduced CBF gradually (to a level of 41 ± 7%). Cortical spreading ischemias were observed 83 ± 42 minutes after onset of superfusion. The DC potential always preceded the CBF decrease (Fig. 6B) or both occurred simultaneously. The DC negativity was −11.1 ± 2.4 mV and the DC shift lasted for 40 ± 25 minutes. The CBF decreased to a level of 14 ± 6% and returned to its level before onset of CSI after 48 ± 25 minutes. One or two CSI events occurred. Three of four animals survived. Hemiparesis was observed in all three animals 24 hours after the experiment (average grade 2.3 ± 0.6). An analysis of tissue samples showed that all three animals had cortical infarction (findings in studies using hematoxylin and eosin, cresyl violet, GFAP, Iba1, and TUNEL staining were similar to those in animals treated

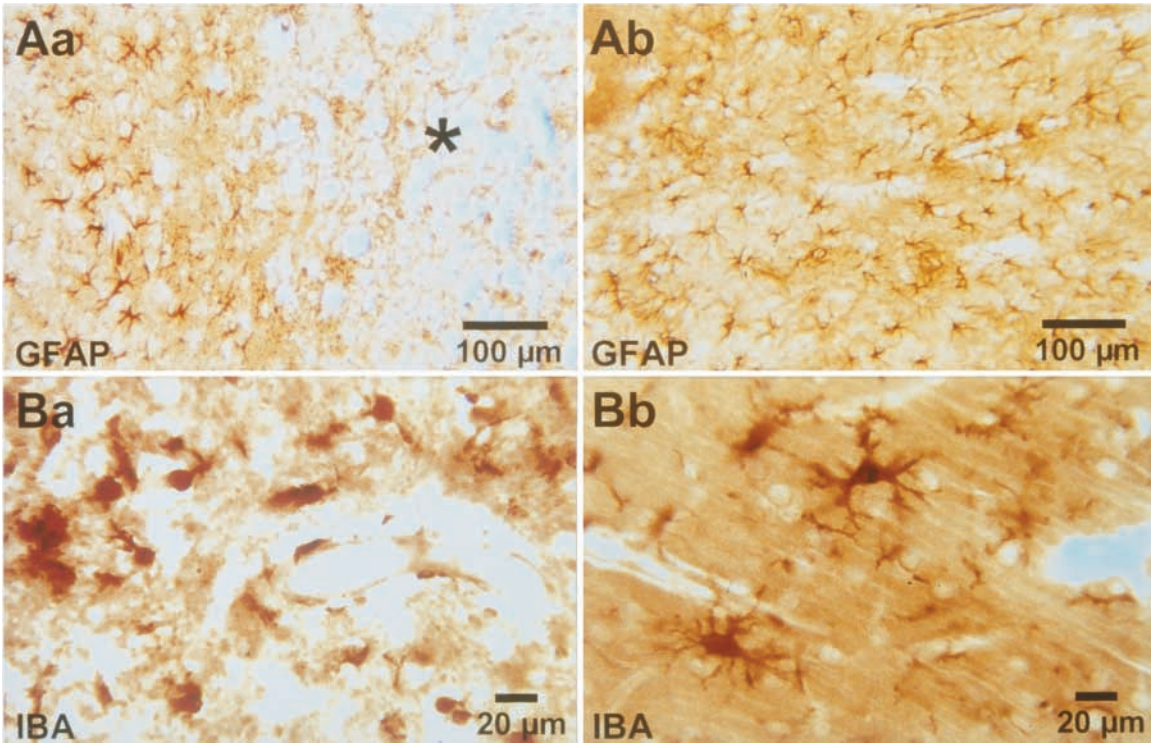

FIG. 5. Photomicrographs Aa: Cortex at the site of the cranial window 48 hours after CSI was induced by Hb (2 mmol/L) and K^+ (35 mmol/L) in ACSF. The GFAP staining reveals loss of astrocytes confined sharply to the infarcted zone *(asterisk)* surrounded by activated astrocytes. Ab: Activated astrocytes in the cortex at the window in a control animal (K^+ [80 mmol/L] in ACSF without Hb) 48 hours after the experiment. GFAP staining. Ba: Larger numbers of phagocytic microglia and other macrophages are observed in the infarcted area 48 hours after CSI (Hb [2 mmol/L] and K^+ [35 mmol/L] in ACSF). Iba1 staining. Bb: Activated microglial cells residing in cortex at the site of the cranial window in a control animal (K^+ [80 mmol/L] in ACSF without Hb) 48 hours after the experiment. Iba1 staining.

with ACSF containing Hb [2 mmol] combined with K^+ [35 mmol/L] and glucose [physiological level]). A coronal section including the window area is shown in Fig. 7A. Higher magnification of this tissue revealed necrosis at the site of the cranial window and neighboring areas (Fig. 7C).

Control Animals

Artificial CSF containing Hb combined with physiological levels of both K^+ and glucose reduced CBF to 44 ± 7% (three animals). No CSI occurred during the observation period, which lasted 3 hours.

Artificial CSF containing increasing concentrations of K^+ (35, 50, and 80 mmol/L) without Hb increased CBF to 169 ± 47% (five animals). No CSDs occurred in response to ACSF with K^+ at concentrations of 35 and 50 mmol/L. There were 6 ± 4 CSDs associated with short initial hypoperfusions followed by hyperemia that were induced with a K^+ concentration of 80 mmol/L (Fig. 8A). The DC potential either preceded the CBF decrease or both occurred at the same time (Fig. 8B). The amplitude of the DC shift was −7.1 ± 1.7 mV. It lasted for 1.1 ± 0.5 minutes. The initial hypoperfusion lasted for 0.8 ± 0.2 minutes. The CBF decreased from 169 to 83 ± 19% followed by short-term spreading hyperemia (CBF level 219 ± 71%).

Artificial CSF containing glucose (0.8 mmol/L) without Hb had no significant effect on the CBF or the DC potential (three animals).

Each of the 11 control animals survived. No animal demonstrated a neurological deficit. Using light microscopy, no cellular damage could be detected, with the exception of some perineuronal halos in the most superficial layer at the window (11 animals). A few TUNEL-positive cells were present in this layer (seven animals). A coronal section including the cranial window area is shown in Fig. 7B. Brain herniation at the window site also occurred in the control animals; however, normal parenchymal structures were preserved (Fig. 7D). Activated astrocytes (Fig. 5Ab) and activated microglial cells (Fig. 5Bb) were observed in both hemispheres without confinement to the window area (seven animals).

Discussion

Histological Findings

Cortical spreading ischemia in response to a superfusion of ACSF with Hb combined with either a high concentration of K^+ or a low concentration of glucose led to characteristic morphological changes. Necrosis in tissue at the site of the cranial window and in neighboring areas was demarcated sharply after 24 hours. After 48 hours, the tissue texture of the core was lost (Fig. 7C). Neurons

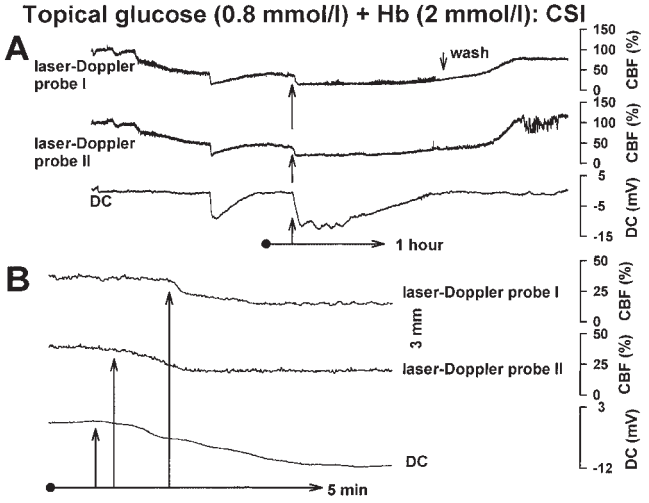

FIG. 6. A: Traces obtained during superfusion of Hb (2 mmol/L) combined with glucose (0.8 mmol/L) in ACSF containing a physiological concentration of K^+. Data from a complete experiment are shown. Similar to Hb combined with a high concentration of K^+ in ACSF, Hb and a low concentration of glucose in ACSF led to a gradual, pronounced reduction in CBF before CSIs originated in cortex at the site of the cranial window. Two CSIs are observed in this animal during the observation period of 3 hours. The first CSI event is shorter than the second. The onset of the second CSI event is indicated by the *arrows*. It lasted for approximately 1 hour. Note the waveform of the negative shift in DC, which represents multiple cycles of CSD (compare with Fig. 1). B: Higher temporal resolution of the second CSI event. Note that the DC shift precedes the CBF decrease.

deemed necrotic, by using hematoxylin and eosin and vanadium acid fuchsin–toluidine blue in histochemical studies, and TUNEL-positive cells and fragments were most abundant in the outer zone of damage after 48 hours. The TUNEL staining did not allow differentiation between necrosis and apoptosis (Fig. 4C), and electron microscopy was not performed. However, according to the criteria of light microscopy, necrosis was much more prominent than apoptosis (Fig. 4C).[14,23] Large numbers of phagocytic microglia and other macrophages were observed in the area of damage where the astrocytes were lost. In other parts of both hemispheres, activated microglia and astrocytes were found compared with naive animals. A rough estimation of infarct sizes revealed pronounced heterogeneity, which is likely to result from the heterogeneity of CSI with respect to the amplitudes of the CBF decrease, duration, frequency, and spatial distribution.

In the contol animals, no significant cellular damage was seen, apart from some TUNEL-positive cells at the surface of the brain. Glial cells are sensors for pathological events. Immunohistochemical detection of astrocyte and microglial activation is therefore a sensitive technique to study subtle pathomorphological reactions. In control animals activated microglial cells and astrocytes were detected in both hemispheres. The bilateral activation may be related to preparation of the cranial window, which produced a meningeal reaction in both hemispheres in all animals.

In summary, CSI has been described as a condition in which ischemia is produced by a vasoconstrictive stimu-

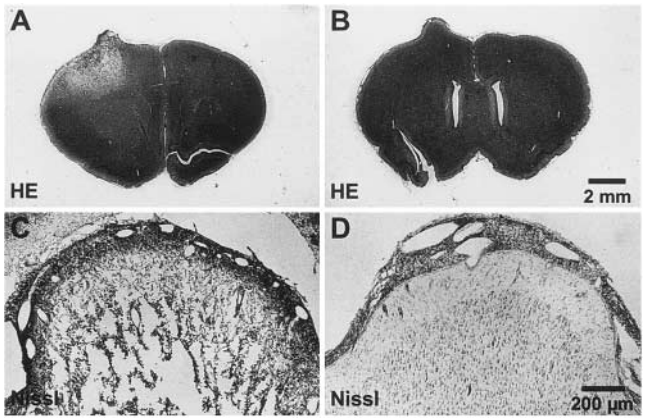

FIG. 7. A: Photomicrograph of a brain tissue sample showing CSI after superfusion of ACSF containing Hb (2 mmol/L) and glucose (0.8 mmol/L) induced cortical infarction. A coronal section including the window area demonstrates focal cortical necrosis 48 hours after CSI. H & E. B: No CSI is observed after superfusion of ACSF containing Hb (2 mmol/L) combined with physiological concentrations of K^+ and glucose. Brain herniation into the cranial window is observed, similar to that seen in A, but there are no signs of necrosis 48 hours after the experiment. H & E. C: Higher-magnification photomicrograph of the window area in A demonstrating destruction of the parenchyma after CSI. Nissl staining. D: Higher-magnification photomicrograph of the window area in B revealing a normal cortical structure in the control animal, although brain herniation and a meningeal reaction are also present. Nissl staining.

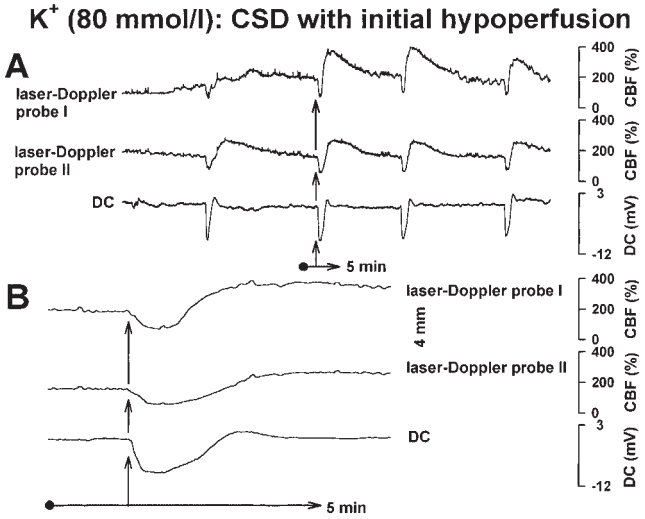

FIG. 8. A: Traces showing initial hypoperfusions followed by cortical spreading hyperemia induced by superfusion of ACSF with K^+ (80 mmol/L) but without the NO scavenger Hb. Interestingly, similar responses to CSD with initial hypoperfusion are also known to result from lowering the concentration of NO and from physiological concentrations of K^+ in ACSF.[11] The *arrows* indicate the onset of the second CSD. B: Higher temporal resolution of the second CSD. Note that the negative shift in DC and the decrease in CBF start almost simultaneously in this experiment. Different temporal relationships between DC negativity and the CBF response within animals and between different animals result from varying initiation sites of CSD in the window. However, similar to CSI and in contrast to anoxic and periinfarction depolarizations, the CBF decrease never precedes the negative DC shift (see *Discussion*).

lus from the neuronal–glial network.[9] Thus, it occurs as the result of a disturbed coupling between brain metabolism and CBF.[9] Within the methodological limits of this study, the histopathomorphological changes after CSI do not differ from those of focal cerebral ischemia, which occurs in response to other conditions such as embolism or thrombosis.[14,23,44]

Delayed Ischemic Neurological Deficits After SAH

Given that lysis of erythrocytes in the subarachnoid space peaks 7 days after SAH at the time of maximum vasospasm, and that DINDs coincide with this process, a causal relationship between factors released by hemolysis and DINDs is postulated (see reviews by Macdonald and Weir[26] and Zabramski[49]). Three prominent extracellular changes that occur during the course of hemolysis are consumption of glucose and increases in Hb and K^+. Using two different combinations of these factors, we produced CSI and brain infarction in rats in this study, suggesting a link between spreading ischemia and DINDs.

Hemoglobin is considered to be the most important factor for the generation of DINDs.[26,49] It has a concentration of 21 mmol/L in the erythrocyte. The subarachnoid level of Hb reaches its maximum on the 7th day after SAH.[40] The reported values range from 500 μmol/L in a subarachnoid hematoma[37] to 100 μmol/L in the perivascular space of the middle cerebral artery[40] and 30 μmol/L in cerebrospinal fluid.[37,48] The Hb concentration applied in our experiments was four times higher than that measured in human subarachnoid blood clots. The rationale for the higher experimental Hb concentration was to achieve statistically unequivocal results: CSI developed in 100% and necrosis in 86% of the animals after the ischemic event. Thus, the response rate to the experimental treatment was considerably higher than the rate of DINDs after SAH in humans who do not receive therapy (20–30% of SAH patients).[19] In addition, the incubation time of Hb during the experiment was shorter compared with that of SAH.

There are only a small number of studies in which the role of K^+ in the generation of DINDs has been investigated. However, K^+ has a high concentration of 100 mmol/L in the erythrocyte. Ohta, et al.,[36] found that, after a delay, extracellular K^+ increased from 3 to 50 mmol/L in intracerebral hematomas in neurosurgical patients.

Decreases in intracortical extracellular glucose (normal range 1–3 mmol/L) are currently being investigated in bedside microdialysis studies of patients after SAH.[34,42] The clinical concentration ranges and time courses suggest that the combination of low glucose and Hb may be more relevant for the development of DINDs than the combination of high K^+ and Hb.[34,36,42] However, the available data are insufficient to correlate precisely the experimental and clinical conditions. In addition, further spreading depression–inducing factors, such as glutamate[2,15,20–22,34,42,43] and hyponatremia,[7,17] need to be investigated in future studies.

The localization of necrosis after CSI in rats is similar to that of DINDs in humans.[33,46] In more than 90% of cases, the substrates of DINDs are cortical infarcts. The histological features of the lesions observed after DINDs and CSI are alike. An example of the spongiform changes in the perivascular region after CSI is shown in Fig. 4A. An almost identical picture was presented by Neil-Dwyer, et al.,[33] to illustrate histological changes after DINDs in humans (Fig. 2 in the article by Neil-Dwyer, et al.).

In summary, the spreading ischemia hypothesis of DINDs is based on two conditions after SAH. One condition is a decreased threshold for depolarization of the neuronal–glial network by factors such as the low flow state caused by vasospasm,[4,32,49] low concentration of extracellular glucose,[1,34,42,50] high concentration of extracellular K^+,[20,36] high concentration of extracellular glutamate,[2,15,20–22,34,42,43] and hyponatremia.[7,17] The second condition is hypothetically a disturbed coupling between the neuronal–glial network and CBF, which means that vasospastic arteries do not respond with dilation but constriction to the depolarization of the neuronal–glial network. Interestingly, CSD-induced ischemia was theoretically proposed as the pathogenesis of migraine stroke.[5,6,9,31] Linking both theories may suggest the presence of migraine as a risk factor for DINDs.

The K^+ Hypothesis of CSI

Little is known about the complex cellular mechanisms involved in spreading ischemia (compare with findings in the report by Dreier, et al.[9]). The depolarization of the neuronal–astrocytic network occurs before or simultaneously with the decrease in CBF during spreading ischemia (compare Figs. 1B, 2B, and 6B). It does not occur after the CBF decrease, in clear contrast with anoxic and periinfarction depolarizations, which follow ischemia induced by mechanical occlusion by approximately 2 minutes.[3,21] The temporal relationship between depolarization and CBF decrease suggests that a vasoconstrictor may be responsible for the CBF decrease, which is released by the neuronal–astrocytic network. The most straightforward candidate is the extracellular K^+ concentration, which increases from 3 to 60 mmol/L early during spreading depression.[16] At this concentration, K^+ acts as a strong vasoconstrictor.[28] Under physiological conditions, the vasoconstrictive effect of the spreading depression–induced rise in extracellular K^+ concentration may be antagonized by NO, because CSI occurs if either the NO scavenger[12,45] Hb or the NOS inhibitor L-NNA is present in the subarachnoid space.[9] With respect to interactions between K^+ and NO, it has been reported that a decrease in NO increased the vasoconstrictive power of a high concentration of extracellular K^+ in dog basilar arteries in vitro.[30] The NO scavenger Hb accentuated vasoconstriction by a high concentration of extracellular K^+ in guinea-pig basilar arteries in vitro.[35] An interactive effect of a moderate K^+ increase in ACSF and NOS inhibition on CBF was shown in the rat in vivo.[10] However, CSI is more pronounced in the presence of Hb than in the presence of L-NNA. This may be explained by additional vasoconstrictive properties of Hb, which include, for example, increased production of vasoconstrictive prostaglandins, lipid peroxides, and endothelin (see review by Macdonald and Weir[26]).

An interaction between K^+ and NO also exists on the level of the neuronal–glial network. Although a threshold of K^+ in ACSF between 20 and 35 mmol/L was shown for the generation of CSD when either Hb or L-NNA were present,[9] the threshold appears to be higher in the absence of an NO-lowering agent in the present study (50–80

mmol/L). A decrease in the K^+ threshold for CSD generation by NO-lowering agents may be due to a decrease in CBF because it may lower K^+ transport by the bloodstream, thus disturbing K^+ release from glial endfeet onto blood vessels.[38] A NO decrease may also lower the K^+ threshold by agonistic effects on NMDA receptor–mediated responses, which have been reported both in vitro[27] and in vivo.[13,39] This is probably due to a decreased NO-mediated downregulatory effect of the redox site of the NMDA receptor complex.[25] The NMDA receptors are involved in the generation and propagation of CSD in all species investigated,[20,22] including rats[15] and humans.[2]

Conclusions

We showed that CSI in the presence of Hb combined with either a high concentration of K^+ or a low concentration of glucose in ACSF in the subarachnoid space led to cortical infarction in the rat.

Acknowledgment

We are grateful to Mrs. Vinogradova for the panoramic photography of the rat brain.

References

1. Astrup J, Norberg K: Potassium activity in cerebral cortex in rats during progressive severe hypoglycemia. **Brain Res 103:** 418–423, 1976
2. Avoli M, Drapeau C, Louvel J, et al: Epileptiform activity induced by low extracellular magnesium in the human cortex maintained in vitro. **Ann Neurol 30:**589–596, 1991
3. Back T, Kohno K, Hossmann KA: Cortical negative DC deflections following middle cerebral artery occlusion and KCl-induced spreading depression: effect on blood flow, tissue oxygenation, and electroencephalogram. **J Cereb Blood Flow Metab 14:**12–19, 1994
4. Back T, Nedergaard M, Ginsberg MD: The ischemic penumbra: pathophysiology, and relevance of spreading depression-like phenomena, in Ginsberg MD, Bogousslavsky J (eds): **Cerebrovascular Disease. Pathophysiology, Diagnosis, and Treatment.** Cambridge, MA: Blackwell Scientific, 1998, pp 276–286
5. Bogousslavsky J, Regli F, Van Melle G, et al: Migraine stroke. **Neurology 38:**223–227, 1988
6. Broderick JP: Stroke and migraine, in Welch KMA, Caplan LR, Reis DJ, et al (eds): **Primer on Cerebrovascular Diseases.** San Diego: Academic Press, 1997, pp 333–335
7. Chebabo SR, Hester MA, Aitken PG, et al: Hypotonic exposure enhances synaptic transmission and triggers spreading depression in rat hippocampal tissue slices. **Brain Res 695:**203–216, 1995
8. Dirnagl U, Kaplan B, Jacewicz M: Continuous measurement of cerebral cortical blood flow by laser-Doppler flowmetry in a rat stroke model. **J Cereb Blood Flow Metab 9:**589–596, 1989
9. Dreier JP, Körner K, Ebert N, et al: Nitric oxide scavenging by hemoglobin or nitric oxide synthase inhibition by N-nitro-L-arginine induce cortical spreading ischemia when K^+ is increased in the subarachnoid space. **J Cereb Blood Flow Metab 18:**978–990, 1998
10. Dreier JP, Körner K, Görner A, et al: Nitric oxide modulates the CBF response to increased extracellular potassium. **J Cereb Blood Flow Metab 15:**914–919, 1995
11. Duckrow RB: A brief hypoperfusion precedes spreading depression if nitric oxide synthesis is inhibited. **Brain Res 618:** 190–195, 1993
12. Edwards DH, Byrne JV, Griffith TM: The effect of chronic subarachnoid hemorrhage on basal endothelium-derived relaxing factor activity in intrathecal cerebral arteries. **J Neurosurg 76:** 830–837, 1992
13. Ferraro G, Montalbano ME, La Grutta V: Nitric oxide and glutamate interaction in the control of cortical and hippocampal excitability. **Epilepsia 40:**830–836, 1999
14. Garcia JH, Liu KF, Ho KL: Neuronal necrosis after middle cerebral artery occlusion in Wistar rats progresses at different time intervals in the caudoputamen and the cortex. **Stroke 26:** 636–643, 1995
15. Gorelova NA, Koroleva VI, Amemori T, et al: Ketamine blockade of cortical spreading depression in rats. **Electroencephalogr Clin Neurophysiol 66:**440–447, 1987
16. Hansen AJ, Quistorff B, Gjedde A: Relationship between local changes in cortical blood flow and extracellular K^+ during spreading depression. **Acta Physiol Scand 109:**1–6, 1980
17. Hasan D, Wijdicks EFM, Vermeulen M: Hyponatremia is associated with cerebral ischemia in patients with aneurysmal subarachnoid hemorrhage. **Ann Neurol 27:**106–108, 1990
18. Imai Y, Ibata I, Ito D, et al: A novel gene *iba1* in the major histocompatibility complex class III region encoding an EF hand protein expressed in a monocytic lineage. **Biochem Biophys Res Commun 224:**855–862, 1996
19. Kassell NF, Torner JC, Haley EC Jr, et al: The International Cooperative Study on the timing of aneurysm surgery. Part 1: Overall management results. **J Neurosurg 73:**18–36, 1990
20. Lauritzen M: Pathophysiology of the migraine aura. The spreading depression theory. **Brain 117:**199–210, 1994
21. Lauritzen M, Hansen AJ: The effect of glutamate receptor blockade on anoxic depolarization and cortical spreading depression. **J Cereb Blood Flow Metab 12:**223–229, 1992
22. Lauritzen M, Rice ME, Okada Y, et al: Quisqualate, kainate and NMDA can initiate spreading depression in the turtle cerebellum. **Brain Res 475:**317–327, 1988
23. Li Y, Sharov VG, Jiang N, et al: Ultrastructural and light microscopic evidence of apoptosis after middle cerebral artery occlusion in the rat. **Am J Pathol 146:**1045–1051, 1995
24. Lillie RD (ed): **Histopathologic Technic and Practical Histochemistry, ed 3.** New York: Blakiston, 1965
25. Lipton SA, Choi YB, Pan ZH, et al: A redox-based mechanism for the neuroprotective and neurodestructive effects of nitric oxide and related nitroso-compounds. **Nature 364:**626–632, 1993
26. Macdonald RL, Weir BKA: A review of hemoglobin and the pathogenesis of cerebral vasospasm. **Stroke 22:**971–982, 1991
27. Manzoni O, Prezeau L, Marin P, et al: Nitric oxide-induced blockade of NMDA receptors. **Neuron 8:**653–662, 1992
28. McCulloch J, Edvinsson L, Watt P: Comparison of the effects of potassium and pH on the calibre of cerebral veins and arteries. **Pflügers Arch 393:**95–98, 1982
29. Menzies SA, Hoff JT, Betz AL: Middle cerebral artery occlusion in rats: a neurological and pathological evaluation of a reproducible model. **Neurosurgery 31:**100–107, 1992
30. Minato H, Hashizume M, Masuda Y, et al: Modulation of extraluminally induced vasoconstrictions by endothelium-derived nitric oxide in the canine basilar artery. **Arzneimittelforschung 45:**675–678, 1995
31. Moen M, Levine SR, Newman DS, et al: Bilateral posterior cerebral artery strokes in a young migraine sufferer. **Stroke 19:**525–528, 1988
32. Nedergaard M, Astrup J: Infarct rim: effect of hyperglycemia on direct current potential and [^{14}C]2-deoxyglucose phosphorylation. **J Cereb Blood Flow Metab 6:**607–615, 1986
33. Neil-Dwyer G, Lang DA, Doshi B, et al: Delayed cerebral ischaemia: the pathological substrate. **Acta Neurochir 131:** 137–145, 1994
34. Nilsson OG, Brandt L, Ungerstedt U, et al: Bedside detection of brain ischemia using intracerebral microdialysis: subarachnoid

hemorrhage and delayed ischemic deterioration. **Neurosurgery 45:**1176–1184, 1999
35. Nishiye E, Nakao K, Itoh T, et al: Factors inducing endothelium-dependent relaxation in the guinea-pig basilar artery as estimated from the actions of haemoglobin. **Br J Pharmacol 96:** 645–655, 1989
36. Ohta O, Osaka K, Siguma M, et al: Cerebral vasospasm following ruptured intracranial aneurysms, especially some contributions of potassium ion released from subarachnoid hematoma to delayed cerebral vasospasm, in Bevan JA (ed): **Vascular Neuroeffector Mechanisms.** New York: Raven Press, 1983, pp 353–358
37. Ohta T, Kajikawa H, Yoshikawa Y, et al: Cerebral vasospasm and hemoglobins: clinical and experimental studies, in Wilkins RH (ed): **Cerebral Arterial Spasm.** Baltimore: Williams & Wilkins, 1980, pp 166–172
38. Paulson OB, Newman EA: Does the release of potassium from astrocyte endfeet regulate cerebral blood flow? **Science 237:** 896–898, 1987
39. Pelligrino DA, Gay RL III, Baughman VL, et al: NO synthase inhibition modulates NMDA-induced changes in cerebral blood flow and EEG activity. **Am J Physiol 271:**H990–H995, 1996
40. Pluta RM, Afshar JKB, Boock RJ, et al: Temporal changes in perivascular concentrations of oxyhemoglobin, deoxyhemoglobin, and methemoglobin after subarachnoid hemorrhage. **J Neurosurg 88:**557–561, 1998
41. Priller J, Haas CA, Reddington M, et al: Calcitonin gene-related peptide and ATP induce immediate early gene expression in cultured rat microglial cells. **Glia 15:**447–457, 1995
42. Sarrafzadeh AS, Unterberg AW, Lanksch WR: Bedside-microdialysis for early detection of vasospasm after subarachnoid hemorrhage. Case report and review of the literature. **Zentralbl Neurochir 59:**269–273, 1998
43. Säveland H, Nilsson OG, Boris-Möller F, et al: Intracerebral microdialysis of glutamate and aspartate in two vascular territories after aneurysmal subarachnoid hemorrhage. **Neurosurgery 38:**12–20, 1996
44. Spielmeyer W (ed): **Histopathologie des Nervensystems.** Berlin: Springer-Verlag, 1922
45. Stamler JS, Jia L, Eu JP, et al: Blood flow regulation by S-nitrosohemoglobin in the physiological oxygen gradient. **Science 276:**2034–2037, 1997
46. Stoltenburg-Didinger G: Neuropathology of subarachnoid hemorrhage, in Bederson JB (ed): **Subarachnoid Hemorrhage: Pathophysiology and Management.** Park Ridge, IL: American Association of Neurological Surgeons, 1997, pp 41–60
47. Victorov IV, Barskov IV: A method for staining ischemic neurons in the brain and spinal cord. **Pathol Physiol Exp Ther 2:** 53, 1993
48. White RP, Macleod RM, Muhlbauer MS: Evaluation of the role hemoglobin in cerebrospinal fluid plays in producing contractions of cerebral arteries. **Surg Neurol 27:**237–242, 1987
49. Zabramski JM: Vasospasm after subarachnoid hemorrhage, in Bederson JB (ed): **Subarachnoid Hemorrhage: Pathophysiology and Management.** Park Ridge, IL: American Association of Neurological Surgeons, 1997, pp 127–156
50. Zhang ET, Hansen AJ, Wieloch T, et al: Influence of MK-801 on brain extracellular calcium and potassium activities in severe hypoglycemia. **J Cereb Blood Flow Metab 10:**136–139, 1990

Manuscript received October 14, 1999.
Accepted in final form June 5, 2000.
This study was supported by a grant from the Deutsche Forschungsgemeinschaft–Sonderforschungsbereich (No. 507 A1) to Drs. Dreier and Dirnagl, and a grant from the Hermann and Lilly Schilling Foundation to Dr. Dirnagl.
Address reprint requests to: Jens P. Dreier, M.D., Department of Neurology, Charité Hospital, Humboldt University, 10098 Berlin, Germany. email: jens.dreier@charite.de.